



Numerical Study of the Settlement of Rafts on Soft Soils Improved by Small Groups of Stone Columns

D. Ghafarian, S. M. R. Imam*

Department of Civil and Environmental Engineering, Amirkabir University of Technology, Tehran, Iran.

ABSTRACT: Stone column installation is used as an economical, simple, and efficient technique for soft ground improvement to reduce settlements, increase bearing capacity and accelerate the drainage of the foundation soil. While design approaches and analytical methods usually consider the condition of a very large loaded area by using unit-cell models, many practical stone column improvement projects deal with finite or semi-infinite loading areas (e.g. storage tank foundations and road embankments, respectively). In recent years, researchers drew attention to studying the behavior of small groups of stone columns. There are some recommendations in the literature for the prediction of settlements of small groups of stone columns (S_{group}) based on results of unit-cell models (S_{uc}). However, these methods are developed for a specific soft soil or loading condition. This paper presents a relationship for the estimation of the ratio of settlement of a finite-sized stone column supported foundation (SCSF) to the settlement of an infinite group as obtained from a unit-cell model (S_{group}/S_{uc}). The sub-soil and loading conditions are easily taken into account in the proposed relationship. For this purpose, the settlement of a large number of SCSFs having various geometrical and mechanical conditions is investigated using numerical FEM modeling.

Review History:

Received: Jul. 10, 2020

Revised: Sep. 04, 2021

Accepted: Sep. 15, 2021

Available Online: Apr. 06, 2021

Keywords:

Stone column group

Settlement ratio

Unit-cell idealization

Settlement improvement factor

Finite element analysis

1- Introduction

Ground improvement by stone column installation is a widely used technique in the field of soft soil rehabilitation. Many field and laboratory tests as well as numerical studies show that stone columns can efficiently increase bearing capacity and decrease the settlement of foundations [1–5]. Moreover, they can be used for accelerating drainage [6,7], mitigation of liquefaction-induced excess pore pressures [8–10], increasing factor of safety of slopes against failure [11], and decreasing soil pressures on retaining walls [12]. Stone columns can also be used in conjunction with geosynthetic encasement [9,13–15], concrete piles [16], circumferential nails [17], load transfer bars [18], or skirted foundations [19,20].

Many analytical methods developed for calculating the settlement of stone column supported foundations (SCSFs) [21–24] use unit-cell models. These models assume an infinitely large loaded area and due to symmetry, only one stone column together with the native soil for a distance from the centerline of the column equal to half of the center to center spacing of columns is considered. However, many practical applications of stone columns (e.g. road embankments, lightweight structures, or oil tank foundations) include strip (finite in one direction in plan) or rectangular and circular (finite in both directions in plan) loading areas. In recent

years, investigations on the behavior of small groups of SCSFs have drawn more attention in research fields [25–30]. Castro stated that the settlement of small groups of encased and non-encased stone columns beneath rigid rafts can be calculated using a simplified method in which stone columns in the group are replaced by a large diameter central column [29]; however, this method cannot be applied for large groups, and flexible or strip grafts. Lower lateral confinement of central columns in small groups is the key point in dividing SCSFs into small and large groups. In unit-cell condition, lateral displacement of points in mid-distance between the center to center distance of stone columns is restricted, and maximum lateral confinement is provided for the central columns (i.e., the geometric condition is satisfied) [31]. However, due to lateral deformation of the peripheral columns in small groups, reduced confinement is expected for the central columns. In smaller groups, the effect of the peripheral columns on the behavior of the group is more noticeable [26]. On the other hand, propagation of vertical stress in-depth due to surcharge is lower for small groups [30]. The combination of these two effects makes the behavior of small groups of stone columns more complex. Therefore, the use of the unit-cell approach for determining the settlement of small groups would be inaccurate [32].

The effect of group size is evaluated in this study in terms of the ratio of settlement of a group having certain dimensions (S_{group}) to the settlement of an infinite group in

*Corresponding author's email: rimam@aut.ac.ir



unit-cell condition (S_{uc}). Having the settlement of an infinite-sized group of stone column (S_{uc}) obtained from analytical or simple axisymmetric or 3D numerical modeling, the ratio S_{group}/S_{uc} can be used to determine the settlement of a finite-sized group. Some recommendations regarding the determination of S_{group}/S_{uc} (or other parameters used for the determination of the settlement of finite-sized groups based on the settlement of a unit-cell model, a single column, etc.) are available in the literature; however, they are limited to specific conditions (raft shape or rigidity, column encasement condition, soft soil properties, etc.). For example, Balaam [33] proposed a method based on the theory of elasticity for determining an interaction factor that provides the settlement of a column due to the loading of another column at a specified distance. Polous and Mattes [34] presented a chart based on field tests on groups of stone columns which provides the ratio of the settlement of a multi-column group to the settlement of a single stone column. Priebe [21] developed charts for determining S_{group}/S_{uc} for rigid square and strip rafts assuming elastic behavior for the native soil and elastoplastic behavior for the stone columns. Killeen and McCabe [26] derived a closed-form equation for determining the S_{group}/S_{uc} of small groups of stone columns supporting concrete rafts in the Bothkennar site soil. Ng [30] proposed design charts for determining the ratio of S_{group} of floating and end-bearing finite-sized groups to the settlement of related end-bearing stone columns in unit-cell conditions.

In the current study, changes in the ratio S_{group}/S_{uc} are investigated for SCSFs having a wide range of geometrical and mechanical conditions. A general equation having only 3 fitting parameters is proposed, and it is shown that it has a suitable function form for fitting the variation of S_{group}/S_{uc} with B/L_c (raft width to stone column length) for various conditions. In the end, a method for determining the fitting parameters of the equation, based on the variation of settlement of rafts without stone columns ($L_c = 0$) with widths (B) is presented and it is shown that this method can be adjusted for various conditions.

2- Numerical Modeling

Stone column supported foundations (SCSFs) analyzed in the current study are assumed to be placed in a site with soil stratigraphy and material properties obtained from a typical, well-documented soft soil site known as the Bothkennar site located in Scotland. The site soil consists of a marine clay deposit known as Carse clay. Properties of the site soils have been studied widely by Nash *et al.* [35], Hight *et al.* [36], and Allman and Atkinson [37]. This site was selected since it consists of a well-known typical very soft soil for which the improvement effects are significant. Also, it is used by previous researchers in numerical studies of stone column group foundations (e.g. [26,27,38–40]), and it is, therefore, possible to compare the results of the current and previous studies. Stratigraphy and mechanical properties of soil layers of this site are introduced in sec. 2.3. Settlement of concrete and granular strip and square rafts, and unit-cell idealization for infinite groups of ordinary stone columns (OSC) and

geosynthetic encased stone columns (GESC) are investigated using FEM modeling. Settlement results are presented in this paper in the form of settlement improvement factor (SIF), which is the ratio of settlement of a raft without columns to an SCSF, and the settlement ratio (S_{group}/S_{uc}), which is the ratio of settlement of a finite-sized group of stone columns to that of the infinite group (unit-cell model) with all other parameters being the same.

2- 1- General

The commercial finite element code Plaxis 3D 2016 [41] is used in this study for numerical analysis of the settlement of SCSFs. Tetrahedral iso-parametric 10-node volumetric elements with 4 Gaussian points were used for modeling the soil, the stone columns, and the raft in the current study. Geogrid elements available in the Plaxis 3D 2016 program were used to model the stone column encasement, where necessary. These are triangular 6-node planar elements, which can resist in-plane tensile stresses but have no bending moment or shear stresses. Numerous researchers have indicated that no interface elements need to be used between the soft soil and the non-encased or geogrid-encased stone columns since field observations have shown that sufficient interlocking occurs between them (see e. g. [25], [27], [29], [42]). Therefore, in the current study, no interface element is considered between soil and stone column or encasement. Due to symmetry in the geometry and loading condition of square and unit-cell models, only one-quarter of the problem domain was modeled. For the strip rafts, each numerical model was taken to have a width equal to half of the center to center distance of the columns. The horizontal dimension of strip and square raft models are selected 4 times the raft size to minimize boundary effects (as suggested by [43]). For unit-cell models, the horizontal dimensions of models are equal to half of the center to center distance of the columns. The depth of numerical models in all analyses is selected to be 14 m below the raft. All vertical sides of the model are fixed for horizontal displacements and the bottom of the model is fixed for displacements in all directions. Fig. 1 illustrates unit-cell, strip, and square raft models.

The numerical modeling procedure consists of three steps. In-situ stresses existing in the soft soil before column installation are generated in the first step. In the second step, the columns are installed (i.e. material of the native soil in the stone column regions is changed to stone column material) and the raft is placed. In this step, stress changes in the native soil due to differences in stone column and native soil gravity loads are calculated. A drained loading stage is then included in the third step to calculate the long-term settlement of the raft under a typical service load, which is considered to be 50 kPa in the current study. It is worth noting that post-installation lateral earth pressure coefficients of the native soil, (K_h^*), are assumed to be the same as those recommended by Killeen and McCabe [26] for different layers of the Bothkennar site soil. The use of elevated lateral earth pressure coefficient (K_h^*) is a common way to take into account stone column installation effects as used by Priebe [21], Watts *et al.* [44],

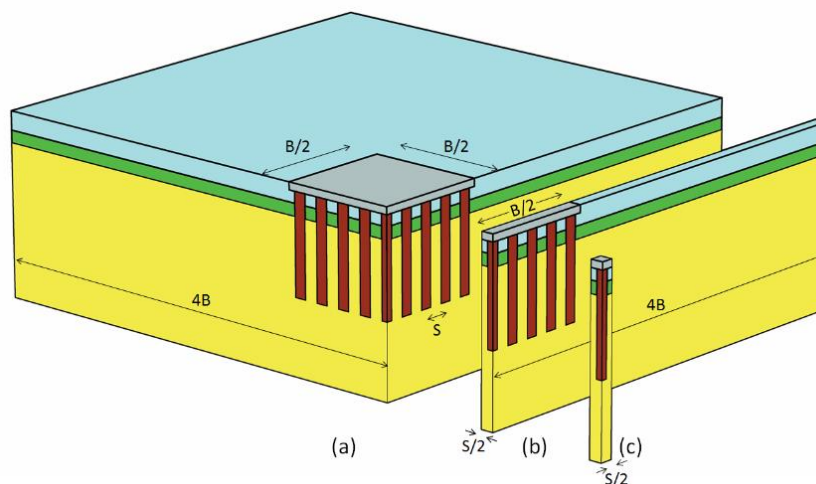


Fig. 1. Typical geometry of numerical models. (a) Square raft, (b) strip raft, and (c) unit-cell model.

Table 1. Mechanical parameters for the stone columns, and the granular and concrete rafts.

| Material | γ (kN/m ³) | Elasticity Modulus (MPa) | | | ϕ' (deg.) | c' (kPa) |
|---------------|-------------------------------|--------------------------|----------------|-----------|----------------|------------|
| | | E_{50}^{ref} | E_{ur}^{ref} | P^{ref} | | |
| Stone Column | 19 | 70 | 210 | 0.1 | 45 | 2 |
| Granular Raft | 18 | 15 | 45 | 0.1 | 30 | 5 |
| Concrete Raft | 25 | $E = 20000$ | | | - | - |

Elkasabgy [45], Castro [29], and values in the range of 0.7 to 2.0 are typically employed for this coefficient. Moreover, as pointed out by Benmebarak *et al.* [46], results of numerical modeling of column installation using cavity expansion theory show that taking into account column installation effects by only increasing K_h^* provides sufficiently accurate results compared to the case in which both increases in soft soil stiffness and lateral earth pressure coefficient are taken into account.

The hyperbolic non-linear elastoplastic constitutive model is known as the Hardening Soil (HS) [47] model available in the Plaxis program was used to define the behavior of the soil layers, the stone columns, and the granular materials comprising the flexible raft. Many researchers successfully used this constitutive model for the drained behavior of both granular and cohesive materials for numerical modeling of stone column groups (see e. g. [26,29,48]). The concrete raft and encasement materials were modeled using the linear elastic material model. The groundwater table was assumed to be at the ground surface. Table 1 shows the mechanical parameters of the granular and concrete rafts, and the stone column materials, taken as typical values used by many researchers (e.g. Sexton and McCabe [49]). In the case of

GESCs, the columns were considered to be encased over their full length, and the stiffness of the geosynthetic materials was assumed to be $J = E \cdot t = 2500$ kN/m, in which J is stiffness for the unit width of the encasement material, E is its elasticity modulus, and t is its thickness. Typical stiffnesses of encasement materials are in the range of 1000 to 4000 kN/m [50].

2- 2- The soft soil site used in the current study

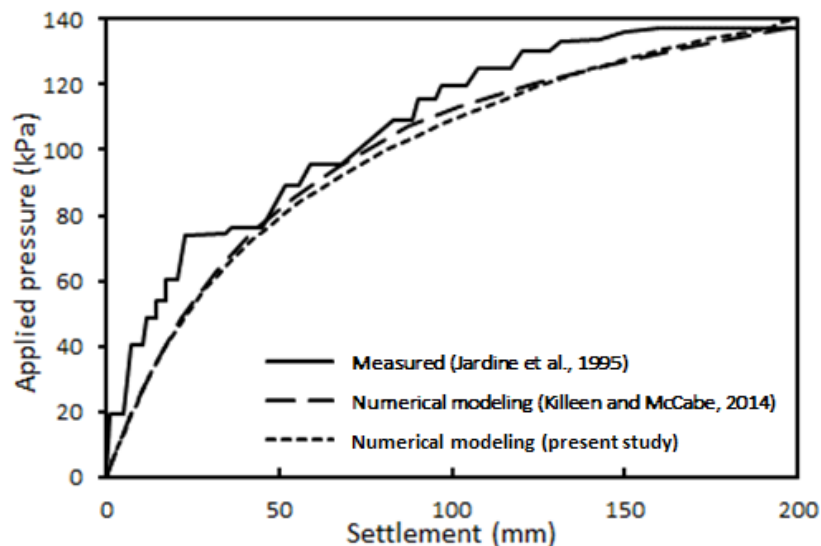
The soil profile of the Bothkennar site is divided into three layers including the crust; upper Carse clay and lower Carse clay. The crust is a shallow 1.5 m thick stiff layer underlain by a softer 1 m thick layer known as the Upper Carse clay and a 12.1 m thick layer of very soft clay known as the Lower Carse clay. Table 2 shows the parameters of the various soil layers present at the Bothkennar site.

2- 3- Numerical model configuration and analysis cases

A large number of three-dimensional finite element analyses were carried out in this study using more than 1500 numerical models of SCSFs to investigate the effects of various factors on their settlement behavior. The stone columns were arranged in square groups consisting of 1, 9,

Table 2. Material parameters for the Bothkennar site soils (after Killeen and McCabe [26]).

| Parameter | Crust | Upper Carse clay | Lower Carse clay |
|----------------------------------|------------|------------------|------------------|
| Depth (m) | 0.0 to 1.5 | 1.5 to 2.5 | 2.5 to 14.6 |
| γ (kN/m ³) | 18.0 | 16.5 | 16.5 |
| E_{50}^{ref} (MPa) | 1.068 | 0.506 | 0.231 |
| E_{ur}^{ref} (MPa) | 5.382 | 3.036 | 1.164 |
| P^{ref} (kPa) | 13 | 20 | 30 |
| m (-) | 1 | 1 | 1 |
| ϕ' (deg.) | 34 | 34 | 34 |
| c' (kPa) | 3 | 1 | 1 |
| K_h^* (-) | 1.5 | 1.0 | 0.75 |
| OCR (-) | 1 | 1 | 1.5 |
| Pre-consolidation pressure (kPa) | 15 | 15 | 0 |

**Fig. 2. Comparison of numerical modeling results with load – settlement curve of a pad footing in Bothkennar site obtained from field load test.**

25, 49, and 81 columns and strip groups having 1, 3, 5, 7, 9, 11, 15, and 21 column rows across their width. For each case, a flexible granular raft and a stiff concrete raft were assumed; and, cases with either geosynthetic encased (GESC) or non-encased stone columns (OSC) were considered. Effects of column length ratio L_c/H (in which L_c is the column length and H is the soft soil thickness), area replacement ratio (A_r), presence of encasement, raft stiffness, and group dimension on the settlement performance of SCSFs was investigated.

2- 4- Numerical Model validation

Validation of the numerical analyses conducted in the current study is done in two steps including 1) validation of soft soil material properties using a full-scale load test on a

shallow raft performed in Bothkennar site soil by Jardine et al [51], and 2) validation of the settlement improvement factors resulting from the numerical modeling of encased and non-encased stone columns in unit-cell condition by comparing them with those calculated using the analytical method developed by Pulko *et al.* [52] which is presented in sec. 3-1-2.

Verification of the HS model parameters adopted for the Bothkennar site soil is done by comparing the load – settlement curve resulting from the field load test performed by Jardine *et al.* [51] on a 0.8 m thick, 2.2 m width square raft without stone. Loading in the field was applied in about 5 days, and the drained condition is considered. A similar validation exercise is used by [26]. Fig. 2 shows a comparison

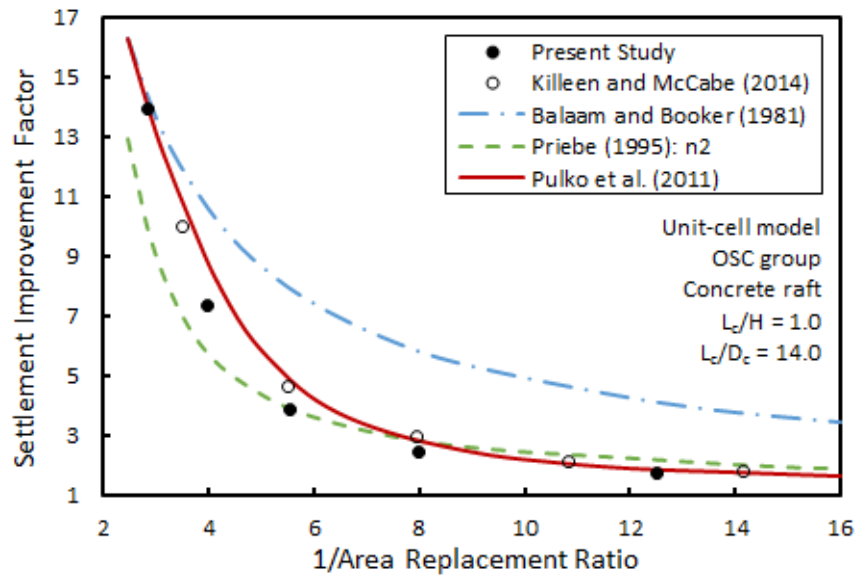


Fig. 3. Comparison of variations of settlement improvement factor with $1/A_r$ obtained in various studies.

of the load-settlement curve in the center point of the pad obtained from field measurements and numerical modeling in this study and those by Killeen and McCabe [26].

3- Results and Discussion

The results of the analyses carried out in the current study are presented and discussed in three parts. In the first part, the settlement improvement factor (SIF) of unit-cell OSC and GESC models having various values of A_r and L_c/H are compared with the SIF obtained from the Pulko *et al.* [52] analytical method, and the validity of the numerical modeling of encased and non-encased columns have been examined. Effects of the width of the strip rafts on the SIF are also discussed. In the second part, the effects of various factors on the settlement ratio (S_{group}/S_{uc}) are studied. A general equation fitted to the numerical results is then proposed and compared with the numerical results obtained for the various cases. In the third part, explanations are provided about how to obtain parameters of the proposed equation for other cases; and, the accuracy of the proposed equation is investigated.

3- 1- Settlement improvement factor

Most analytical methods proposed for calculating the settlement of SCSFs are based on the calculation of the settlement improvement factor (SIF). Examples are the methods proposed by Balaam and Booker [53], Priebe [21], and Pulko *et al.* [52]. These methods are presented for the calculation of SIF of SCSFs in unit-cell conditions and are mainly developed for end-bearing columns; however, with some approximations, they can also be applied for floating columns. In this section, the results of numerical analyses obtained in the current study are first compared with the

above-mentioned analytical methods, and the effects of group size on SIF are then investigated.

3- 1- 1- Effect of area replacement ratio

SIFs for 1.0 m diameter ($D_c = 1.0$) end-bearing OSCs using unit-cell models (i.e. simulating a large group of stone columns) obtained in the current study are compared in Fig. 3 with the values adopted from Sexton *et al.* [48] and Killeen and McCabe [26]. The latter values are calculated using the analytical methods of Priebe [21], Pulko *et al.* [52], and Balaam and Booker [53] and are all obtained for the same sub-soil condition used in the current study. The analytical method presented by Pulko *et al.* [52] is a closed-form elastoplastic extension of Balaam and Booker's [53] elastic method which considers plastic behavior for the stone column material. The Priebe [21] design method is based on assuming elastoplastic behavior for the stone columns and elastic behavior for the surrounding soil and predicts the settlement improvement factor of the SCSFs in unit-cell conditions. The Killeen and McCabe numerical analysis results for the same condition are also provided in Fig. 3. A good agreement generally exists between the results of current numerical modeling and those of Killeen and McCabe [26], and they are also consistent with the results obtained from the analytical methods provided by previous research. However, because of the assumption of elastic behavior for the stone columns by Balaam and Booker [53], their settlement improvement factors are generally overestimated, especially for the lower values of area replacement ratio.

3- 1- 2- Effect of column length and encasement

SIF of concrete rafts resting on floating and end-bearing encased and non-encased 1.0 m diameter stone columns in

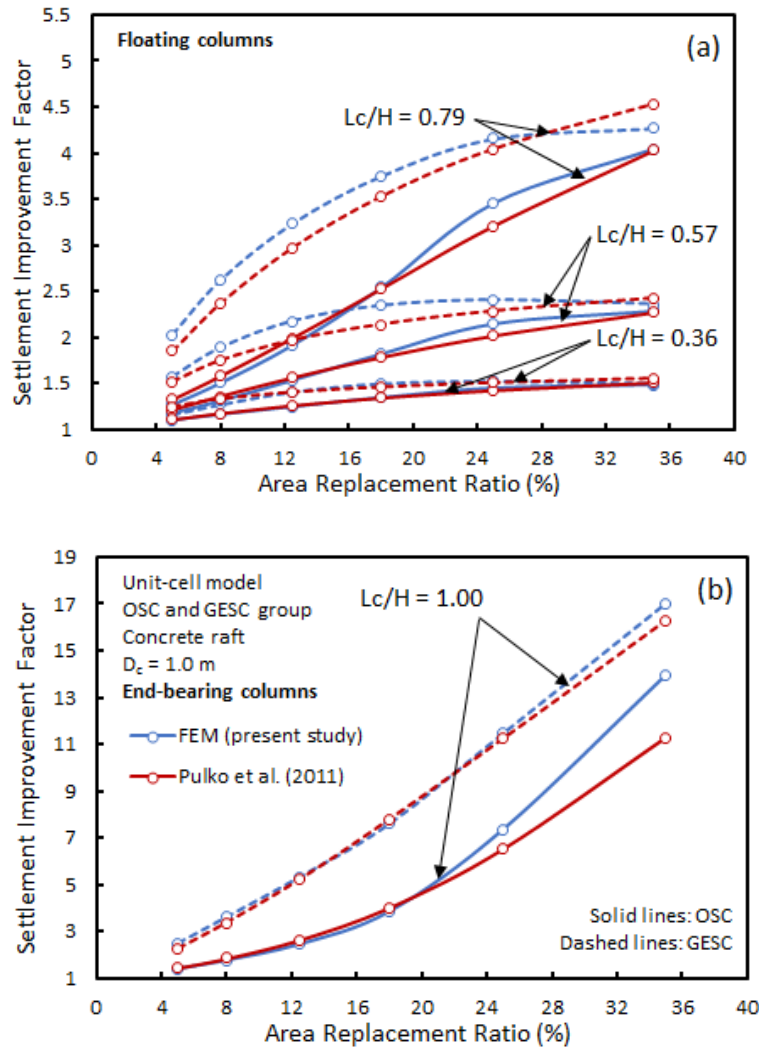


Fig. 4. Comparison of numerical (current study) and analytical (Pulko et al. [52] method) values of SIF for different values of L_c and A_r for OSCs and GESC in unit-cell condition (a) floating column and (b) end-bearing columns.

unit-cell conditions with various values of A_r and L_c/H are shown in Fig. 4 together with the SIF values calculated using Pulko *et al.* [52] analytical method, which has best agreement with numerical modeling results as shown in Fig.3. Due to the various ranges of SIF for floating and end-bearing columns, they are plotted in separate figures. It must be noted that in the Pulko *et al.* [52] method, the soil profile and stone columns are subdivided into 0.1 m thick sub-layers and the material stiffness of each sub-layer is calculated using the stress dependency law ($E = E^{ref} (p/p^{ref})^m$). Since the Pulko *et al.* [52] method was derived for end-bearing stone columns, evaluation of the floating stone columns' SIF is conducted in this study using the native soil material properties rather than the column material properties for sub-layers below the column toe. Although there are some differences between the values obtained from the analytical and the numerical method, especially at high A_r values, a relatively good agreement exists between the analytical method and the results of FEM

modeling for both end-bearing and floating encased and non-encased columns. Sexton *et al.* [48] also observed differences between the SIF obtained from the Pulko *et al.* [52] method and the FEM at high values of A_r , while a good agreement was observed for lower values of A_r . Agreement between numerical modeling results and those calculated based on the analytical method proposed by Pulko *et al.* [52] is considered as verification of the numerical modeling procedure of stone columns in unit-cell conditions. However, SIF values obtained from numerical modeling of strip rafts having various widths (B) as presented in the next section shows that the SIF of large strip rafts asymptotes to unit-cell results, and therefore, numerical modeling of strip groups of stone columns can also be verified.

As shown in Fig. 4, increasing A_r causes the SIFs to increase. However, in floating columns, a limiting value of SIF can be defined such that greater SIF values cannot be achieved by increasing A_r . The limiting SIF value seems to

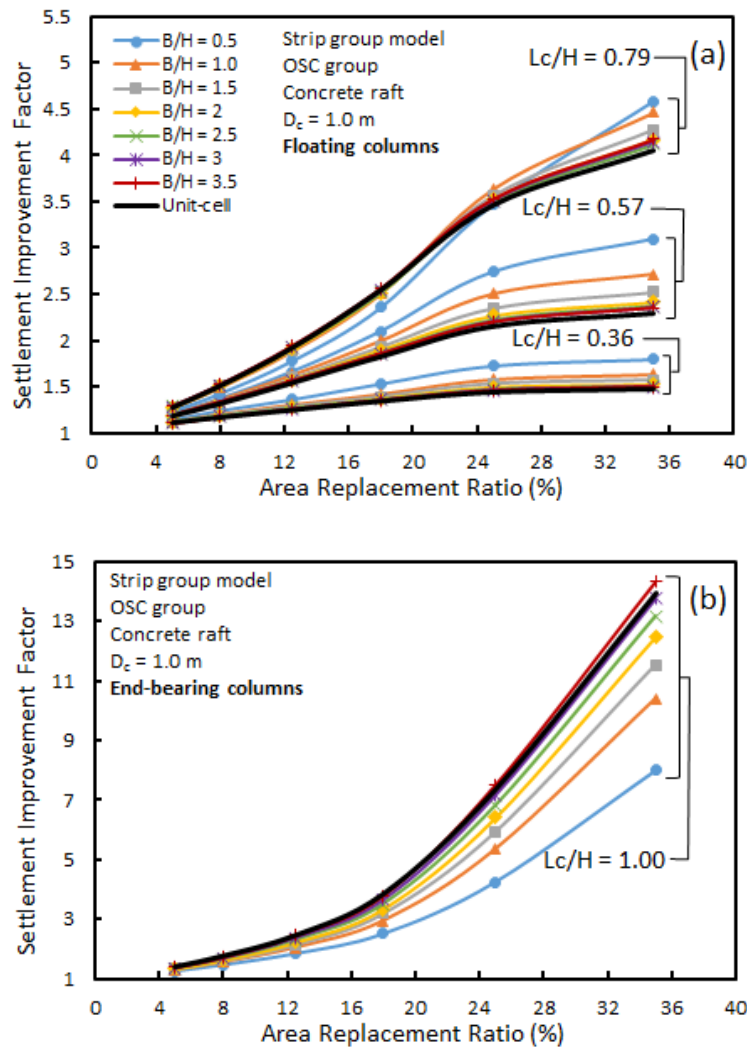


Fig. 5. Effect of width of strip concrete raft supported by groups of OSC on the SIF for (a) floating and (b) end-bearing groups.

be almost the same for OSCs and GESCs for which other parameters are the same. Also, Fig. 4a shows that floating GESCs reach the limiting value of SIF at a smaller A_r compared to OSCs. SIF for end-bearing columns as shown in Fig. 4b continuously increases with an increase in A_r for GESCs and OSCs and there is no limiting value for SIF in end-bearing columns. This behavior is mainly due to the different deformational behavior of end-bearing and floating stone columns as discussed in the following sections.

3- 1- 3- Effect of group width

Settlements of concrete strip rafts having various widths supported by both OSC and GESC with various L_c/H and a diameter of 1.0 m were determined. Fig. 5 shows the effects of group width on the SIF of strip SCSFs consisting of OSCs and Fig. 6 shows similar results for GESCs. According to

these figures, in the case of floating groups, both in OSC and GESC, raft width ratios (B/H) greater than 2 have negligible effects on the SIF. In other words, the settlement at the location of the central columns of the raft in groups with raft width ratios beyond this value is close to the settlement of a large (i.e. infinitely wide) group, and the unit-cell concept is therefore applicable to the determination of the settlement of the interior columns. Similarly, for end-bearing SCSFs, it can also be seen that with the increase in B/H , the SIF converges to the value of the SIF corresponding to the unit-cell condition; however, in this case, the convergence rate is slower in comparison with the floating groups. In the case of end-bearing stone columns, the limiting value of B/H is approximately 3, beyond which raft width no longer affects the results.

It can be seen from Fig. 5 and 6 that in general, the SIF

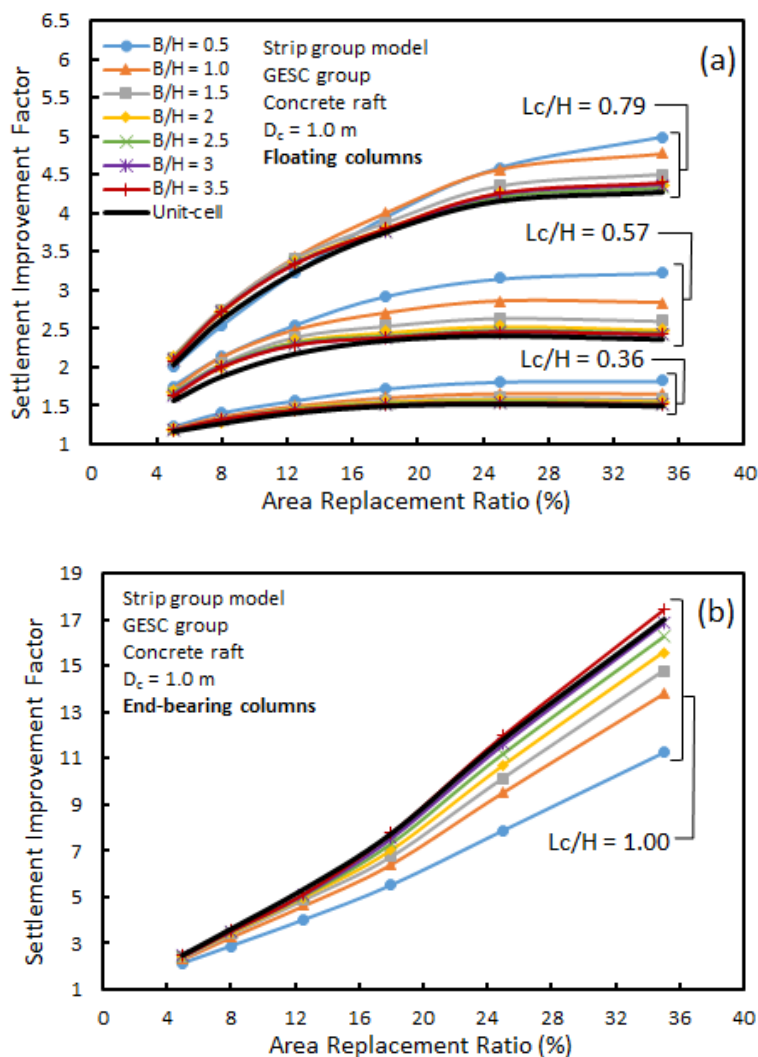


Fig. 6. Effect of the width of strip concrete raft supported by groups of GESC on the SIF for (a) floating and (b) end-bearing groups.

decreases with an increase in B/H of floating column groups; while it increases with the increase in B/H of end-bearing column groups. This behavior can be attributed mainly to the difference in the distribution mechanism of stresses and settlements in the floating and end-bearing SCSFs. Increasing raft width leads to an increase in the magnitude of vertical stress at depth in the soft soil in floating groups; while in the case of end-bearing groups, the vertical stresses are transferred to the bearing layer through the columns. In floating groups, an increase in the stiffness of the improved block due to an increase in the A_r and the higher column confinement due to the use of encasement have limited effects on the SIF, and the raft settlements occur mainly due to settlement of the soil below stone column reinforced block. Therefore, an increase in B/H decreases the settlement improvement factor due to penetration of the vertical stresses to greater depths in the soft

soil as a result of the larger loaded area. However, in the case of end-bearing groups, the settlement depends primarily on the ability of the columns to transfer the loads to the bearing stratum. As the group width increases, more columns in the group will behave as interior columns and will have greater confinement and smaller settlements. In smaller width groups, more columns will be closer to the group perimeter and will have less confinement and higher settlement. Fig. 5(b) and 6(b) show that in end-bearing columns, the effect of group width (B) is more pronounced for higher area replacement ratios, likely due to the greater effect of confinement as column spacing decreases at higher A_r . An increase in A_r or use of encasement, increase the stiffness of the improved block, and this leads to the transfer of a higher proportion of the surface load to the bearing stratum through the stone columns as shown later. In this case, higher confinement can

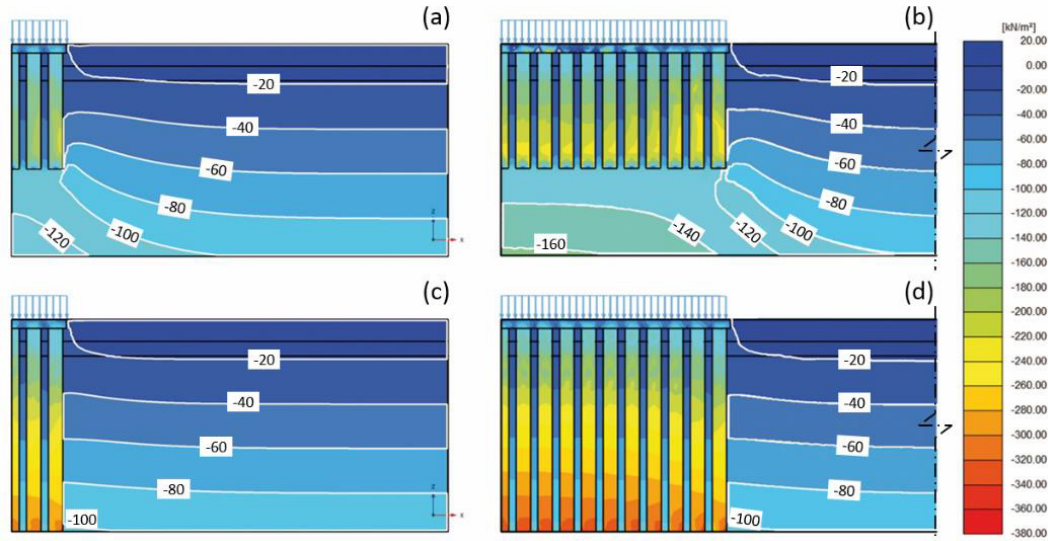


Fig. 7. Effect of group dimension on vertical effective stresses below concrete strip raft models with OSC and (a) $B/H = 0.5$, $L_c/H = 0.57$; (b) $B/H = 2.0$, $L_c/H = 0.57$; (c) $B/H = 0.5$, $L_c/H = 1.00$; (d) $B/H = 2.0$, $L_c/H = 1.00$.

have a greater effect on increasing the SIF.

Fig. 7 shows the distribution of the vertical effective stress in the soil profile for a concrete strip raft supported by a group of OSCs for $A_r = 35\%$ (in which the effect of group dimension is more significant), and for $B/H = 0.54$ and 2.25 . The figure compares results for an end-bearing column group with those for a floating group having $L_c/H = 0.57$. As shown in the figure, vertical stresses in the soil surrounding the columns in the case of end-bearing groups are not much affected by the group width; while in the case of the floating group as shown in Fig. 7(a) and 7(b), the wider raft induces higher vertical stresses in the soft soil. Moreover, a comparison of stress contours inside and outside the end-bearing columns in Fig. 7(c) and 7(d) indicates that a higher proportion of the surface load is transferred by the stone columns in the wider group. This has led to similar stresses (and settlements) experienced by the soft soil, despite the much higher loads applied to the SCSF, and the higher stresses induced in the columns in the larger group. Therefore, in end-bearing groups, the SIF will be higher in the case of a larger group.

Variations of the vertical strains with depth along a vertical line crossing the centerline of the above-mentioned groups are also plotted in Fig. 8a and b, respectively, for floating ($L_c/H = 0.57$) and end-bearing groups ($L_c/H = 1.00$). It must be mentioned that in this figure, vertical strains of floating groups (Fig. 8a) have been shown for stone column-reinforced depth (up to depth -8 m below the raft) and the soil beneath the stone columns (depth -8 m to -14 m below the raft). It can be seen from the figure that increasing B/H from 0.54 to 2.25 in the case of floating columns increased the vertical strains in the regions under the stone columns and that the improved block seems to punch into the underlying soil. In the case of

end-bearing columns, the increase in column stiffness (due to an increase in confinement just below the stiff surficial crust layer) has caused a decrease in the vertical strain of the column for the case with $B/H = 2.25$. The magnitude of the maximum vertical strain at depth for the floating group is about 5 times larger than that for the end-bearing group, and it is located just under the columns. The maximum vertical strain in the end-bearing column groups is located at a depth of about 3m below the raft (about one column diameter below two surficial stiff layers).

3- 2- Settlement ratio of SCSFs

Studying the effect of group dimension as well as other geometrical and mechanical parameters on settlement ratio (S_{group}/S_{uc}) helps extend the readily calculated unit-cell settlements to obtain a settlement of SCSFs with finite dimensions and various conditions. Determination of settlement of such stone column groups often requires time-consuming 3D numerical modeling. Some authors (e.g. Priebe [21] and Killeen and McCabe [26]) suggested charts or equations for determining S_{group}/S_{uc} based on geometrical parameters involved in the problem (B , L_c , D_c , and H). The equation presented by Killeen and McCabe [26] is developed for small square groups of stone columns beneath a concrete raft and it is shown in Eq. (1). Priebe [21] presented two charts for determining S_{group}/S_{uc} as a function of H/D_c for strip and square rafts having a various number of columns considering vertical stress propagation due to loading on small rafts. In the current study, variations of S_{group}/S_{uc} with the various factors are examined using the results of 3D numerical analyses. A close-form relationship, having a general form as Eq. (2) fitted on numerical results of S_{group}/S_{uc} . The general form considered is based on the iterative selection of various

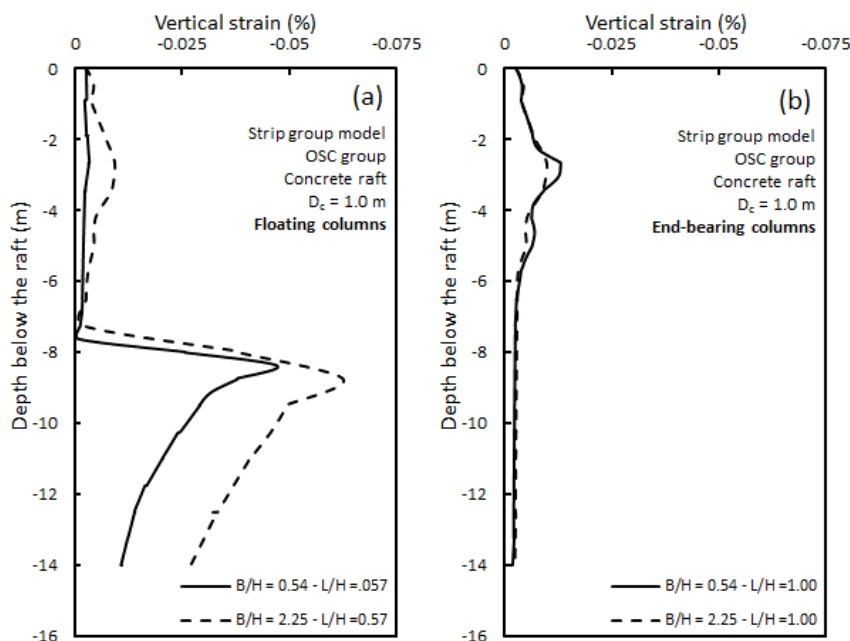


Fig. 8. Effect of group dimension on the vertical strains below concrete strip raft models with OSC (a) floating and (b) end-bearing group.

functions for fitting on numerical results. In the end, it is shown how constant parameters in this equation ($a = f(H/L_c)$, b , and m) can be determined for a specific condition.

$$\frac{S_{group}}{S_{uc}} = \left(0.61 \left(\frac{L_c}{H} \right)^2 + 0.1 \left(\frac{L_c}{H} \right) + 0.06 \right) \cdot \left(\frac{B}{L_c} \right) \quad (1)$$

$$\frac{S_{group}}{S_{uc}} = 1 - \left(1 + \left(\frac{B/L_c}{a} \right)^b \right)^{-m} \quad (2)$$

3- 2- 1- Comparison of S_{group}/S_{uc} from numerical analyses with design charts

Fig. 9 shows results obtained from the current FE analyses presented in the term of S_{group}/S_{uc} compared with those of Priebe [21], obtained using analytical methods, and results provided by Poulos and Mattes [34], which are based on limited field data, which were recommended by Barksdale and Bachus [54] for practical use. Results from the current numerical study shown in the figure were obtained from models with concrete rafts supported by groups of OSC. It is worth noting that for the determination of the Poulos and Mattes [34] values of S_{group}/S_{uc} shown in this figure, their recommended tentative design value of S_{group}/S_{Icol} (in which S_{Icol} is the settlement obtained from a raft on one stone column) for any number of columns has been divided here

by the value of $S_{1000col}/S_{Icol}$ they provided in their chart. In other words, as noted in the Poulos and Mattes [34] original chart, results obtained for a group of 1000 columns ($S_{1000col}$) are considered to be equivalent to those obtained for unit-cell conditions. Also, for comparing the current results with those of Priebe [21], the practical range of the H/D_c ratio used in his charts is considered. The value of H/D_c used in the present numerical analysis results shown in Fig. 9 is equal to 14. The figure shows that results from the Poulos and Mattes [34] chart are relatively consistent with those of the current study for end-bearing groups; while the Priebe [21] results are generally closer to those of the floating groups. The error bars in this figure show the range of settlement ratios for various values of L_c/H in the range of $L_c/H = 0$ to 0.79.

In the current study, the ratio of group width to the column length (B/L_c) is selected for correlation with S_{group}/S_{uc} as suggested by Killeen and McCabe [26]. Various cases with different values of L_c/H , A_r , raft stiffness and shape, encasement condition, and sub-soil stiffness are examined and the effect of B/L_c on the settlement ratio (S_{group}/S_{uc}) is studied for the various cases.

3- 2- 2- Effect of A_r and L_c/H

Fig. 10 shows the variation of settlement ratio (S_{group}/S_{uc}) with the raft width to column length ratio (B/L_c) for various values of column length ratio (L_c/H) and area replacement ratio (A_r). Concrete strip rafts supported by groups of 1.0 m diameter Ordinary (non-encased) stone columns (OSC) are presented in the figure. Results in the figure are for end-bearing ($L_c/H = 1$) and floating ($L_c/H < 1$) OSCs. As shown in

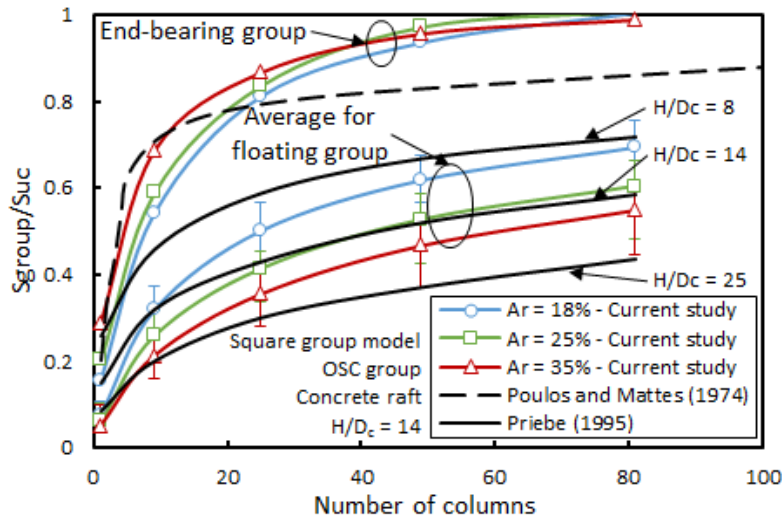


Fig. 9. Comparison of present study results with those of Poulos and Mattes [34] and the Priebe [21] recommended charts (for square group models with $D_c=1.0$ m, OSC, and concrete raft).

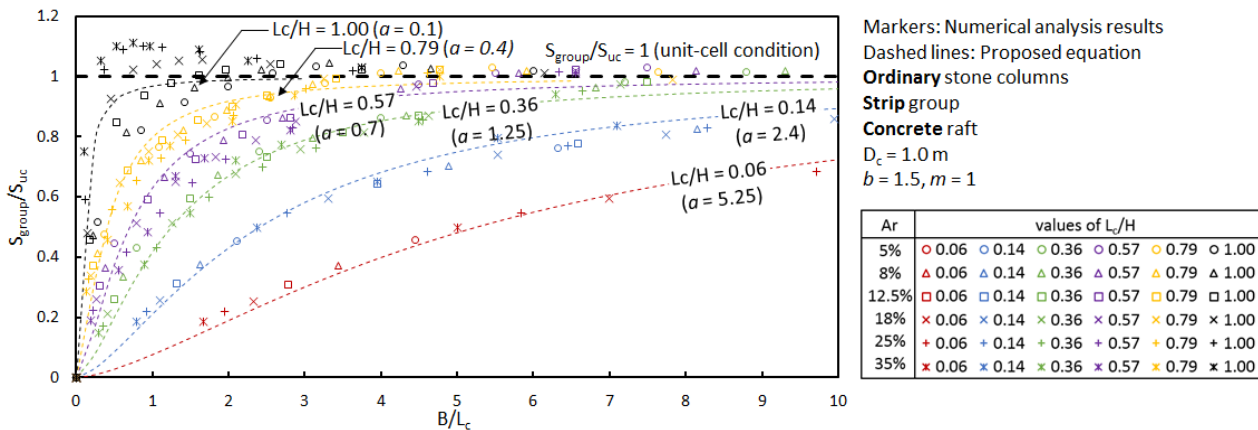


Fig. 10. Effect of L_c and A_r on S_{group}/S_{uc} (OSC strip group with concrete raft).

the figure, S_{group}/S_{uc} generally increases with an increase in B/L_c , and for a sufficiently large raft, it asymptotes to unity. It is shown in this figure that S_{group}/S_{uc} increases as L_c/H increases. Also, it can be seen that S_{group}/S_{uc} is not noticeably influenced by A_r for floating groups (different markers having same color show different A_r values for a specific L_c/H). However, the settlement ratio of end-bearing columns (black markers), increases as the A_r increases. Such scattering in S_{group}/S_{uc} of end-bearing groups having different A_r is also reported by Killeen and McCabe [26]. S_{group}/S_{uc} of end-bearing groups may reach values slightly greater than unity for high A_r ; while, it seems that it asymptotes to unity for large enough

rafts. Elshazly *et al.* [32] stated that in the cases in which end-bearing stone columns are installed in a very weak soft soil, settlement of small groups may exceed the settlement of very large groups (unit-cell condition). They found that this subject is more intense in the case of flexible rafts on end-bearing columns. This issue is discussed more in the following. Predicted values of S_{group}/S_{uc} based on Eq. (2) are also shown in this figure by dashed lines. Parameters a , b , and m are determined based on curve fitting for these cases. It must be noted that parameters b and m are constant for cases presented in Fig. 10 and parameter a varies with L_c/H .

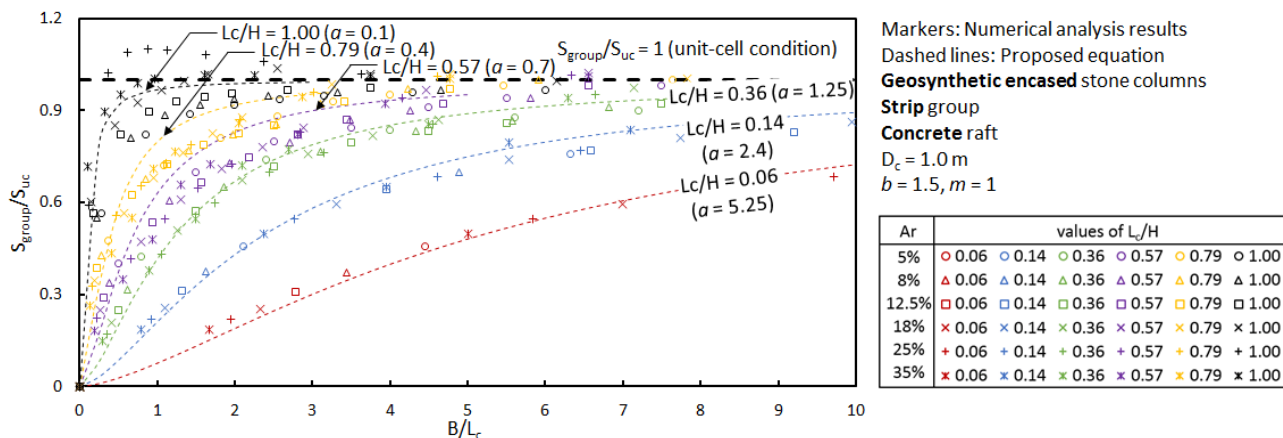


Fig. 11. Effect of column encasement on S_{group}/S_{uc} (GESC strip group with concrete raft).

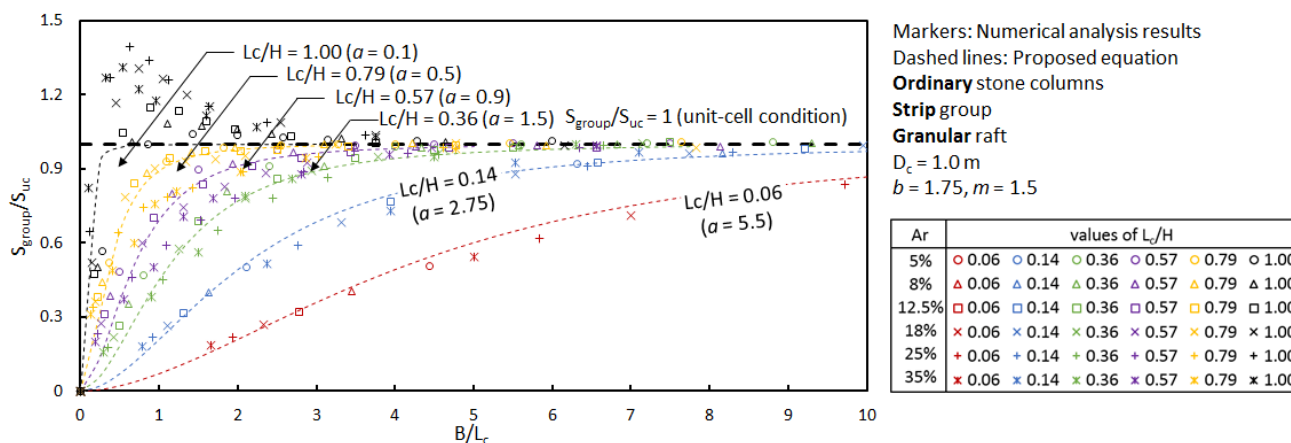


Fig. 12. Effect of L_c and A_r on S_{group}/S_{uc} (OSC strip group with granular raft).

3- 2- 3- Effect of column encasement

Fig. 11 shows the results of S_{group}/S_{uc} of the cases presented in Fig. 10 but for “Geosynthetic encased stone columns” (GESCs). As shown in this figure, almost the same values of curve fitting parameters (a , b and m) as used for OSC groups in a specific condition are applicable for the case of GESC groups and column encasement has a negligible effect on the S_{group}/S_{uc} ; because this ratio is obtained by dividing the settlement of an SCSF with encased stone columns by the settlement of a unit-cell with encased column; and, therefore, the effect of encasement on the settlement ratio somehow cancels out. On the other hand, as it will be shown in the following sections, curve fitting parameters obtained from results of S_{group}/S_{uc} in the case of $L_c = 0$; therefore, they depend on the properties of sub-soil as well as loading condition (strip or square rafts, flexible or rigid rafts) and it is expected that column properties, including column encasement, have minor influence on the S_{group}/S_{uc} of such groups.

3- 2- 4- Effect of raft rigidity

The settlement ratio (S_{group}/S_{uc}) of the cases is presented in Fig. 10 but for “granular raft” supported by ordinary stone columns are presented in Fig. 12. Comparing the results of numerical analyses (markers) presented in Fig. 12 with those presented in Fig. 10 shows that generally decreasing raft rigidity increases S_{group}/S_{uc} ; or in another word, settlement of more flexible rafts is closer to the settlement of unit-cell condition. For example, considering $L_c/H = 0.36$ and $B/L_c = 4$, for concrete raft $S_{group}/S_{uc} = 0.8$ while for granular raft it is almost equal to 1. It can be seen in Fig. 12 that S_{group}/S_{uc} of end-bearing columns for low values of B/L_c in this case (granular raft) is considerably larger than unity (up to 1.4). It means that using unit-cell idealization for the calculation of settlement of end-bearing columns in very soft soils may be considerably underestimated.

Increasing raft width cause: 1) an increase in vertical stress in depth and 2) provide more lateral confinement for

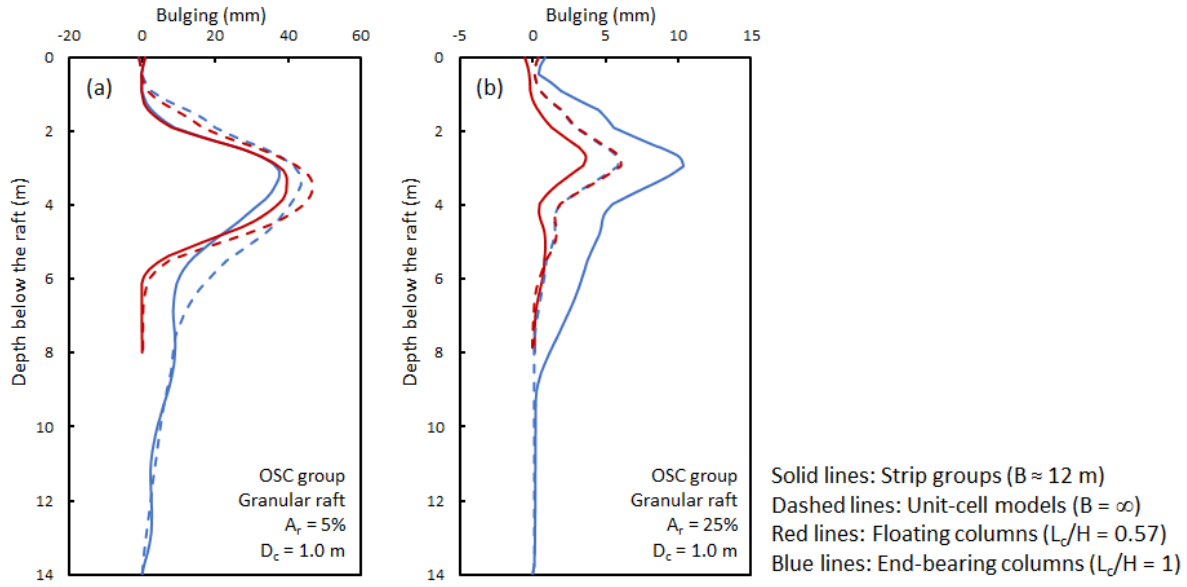


Fig. 13. Effect of A_r and L_c on bulging of central column (a) $A_r = 5\%$ and (b) $A_r = 25\%$.

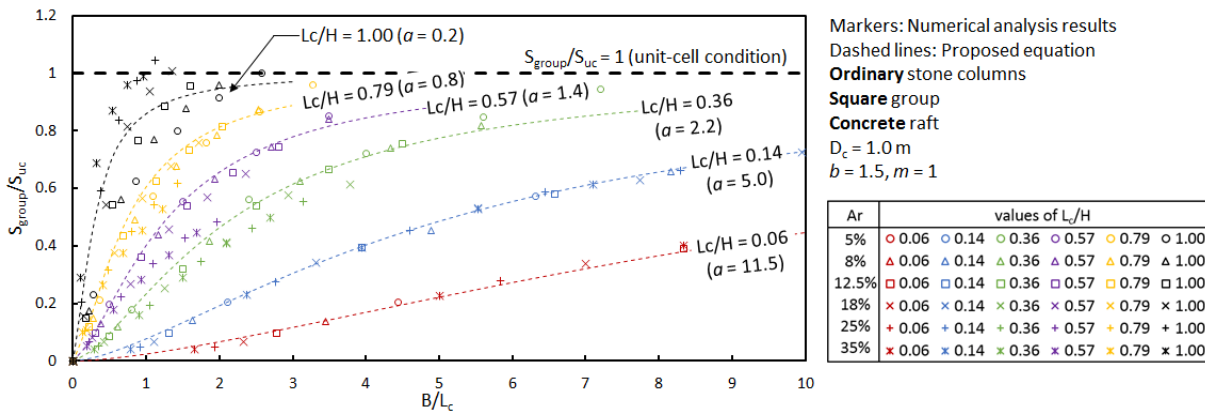


Fig. 14. Effect of L_c and A_r on S_{group}/S_{uc} (OSC square group with concrete raft).

columns as a result of an increase in stress in native soil around columns. The first effect increases the axial force in columns and increases the settlement and the second one increases column stiffness and decreases the settlement. Therefore, it seems that depending on the conditions, one of the mentioned effects may be dominant. A comparison between bulging (lateral displacement in the location of column perimeter) of central column in the case of floating ($L_c/H = 0.57$) and end-bearing ($L_c/H = 1$), closely and widely spaced stone columns ($A_r = 25$ and 5% , respectively) is shown in Fig. 13. Width of raft in these two cases selected as closely as possible ($B = 12.25$ m for $A_r = 25\%$ and $B = 12$ m for $A_r = 5\%$). The case with $A_r = 25\%$ has 7 rows of stone columns and the case with $A_r = 5\%$ has 3 rows of stone columns. It can be seen in this figure that for the case of $A_r = 5\%$ and floating column in the case of $A_r = 25\%$, increasing raft width (from about 12

m to infinity) increases bulging as a result of the first effect mentioned above; however, for an end-bearing column having $A_r = 25\%$, the second effect is dominant (bulging of the central column with $B = 12$ m is greater than bulging of the column in unit-cell condition). Since increasing bulging, increases the settlement of the raft, and the settlement of the central point of a flexible raft is most controlled by the settlement of central columns, it is reasonable that the settlement of small groups of closely spaced end-bearing stone columns may be more than unit-cell condition.

3- 2- 5- Effect of raft shape

The settlement ratio (S_{group}/S_{uc}) of the cases is presented in Fig. 10 and Fig. 12 but for the “square raft” supported by ordinary stone, columns are presented in Fig. 14 and Fig. 15. Comparing numerical results (markers) of S_{group}/S_{uc} for cases

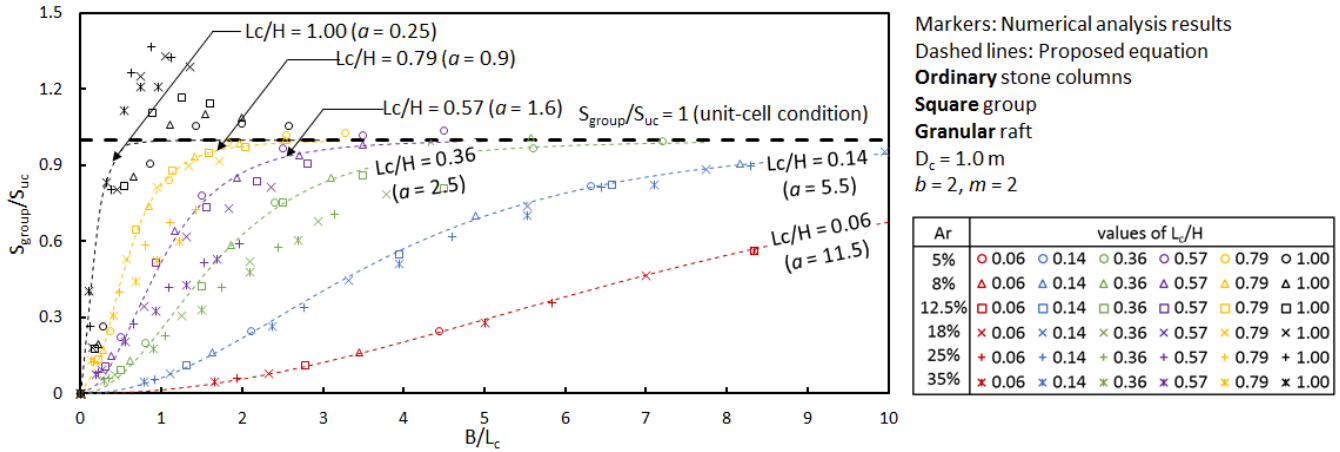


Fig. 15. Effect of L_c and A_r on S_{group}/S_{uc} (OSC square group with granular raft).

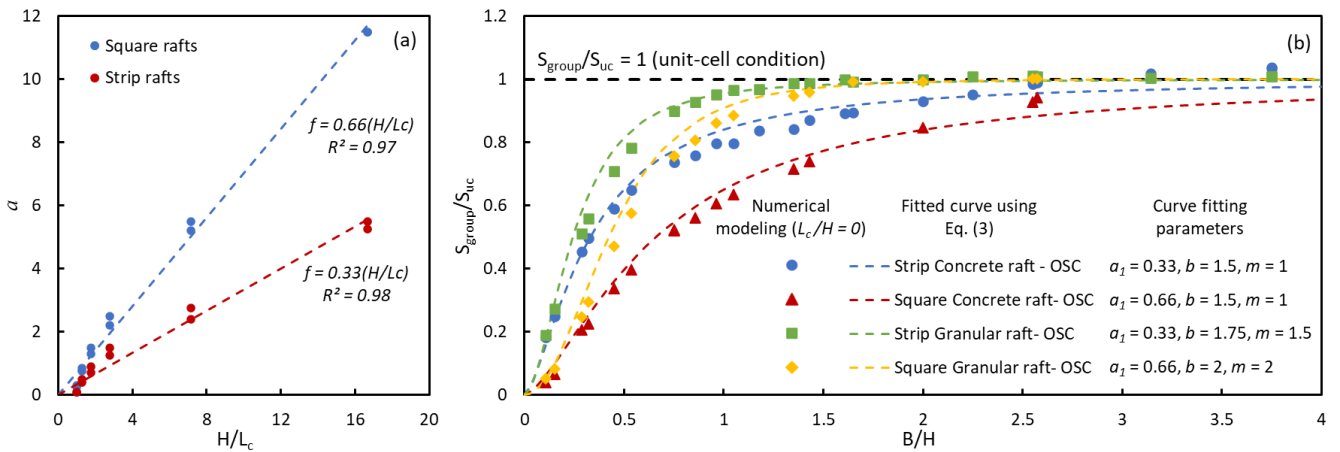


Fig. 16. Determination of curve fitting parameters for square and strip, concrete and granular rafts in Bothkennar soil profile (a) determination of a and (b) determination of parameters b and m .

having square rafts with related cases having strip rafts shows that increasing raft dimension ratio (B/L_c : ratio of raft width to its length) from 0 (for strip raft) to 1.0 (for square raft) decreases the S_{group}/S_{uc} and the tendency of strip rafts to reach unit-cell condition ($S_{group}/S_{uc} = 1$) is greater than the square rafts. This is because strip raft size is infinite in one direction; and, under the same conditions, stresses and settlements in the soil mass under a strip raft are closer to those corresponding to the unit-cell condition (infinite in both directions) compared to square rafts. For example, for the case of the concrete raft and $L_c/H = 0.36$ (green markers) and $B/L_c = 5$, the value of S_{group}/S_{uc} of the strip raft (Fig. 10) is near 1 while for the square raft (Fig. 14) S_{group}/S_{uc} is about 0.7. Predicted values of S_{group}/S_{uc} based on Eq. (2) are also shown in these figures by dashed lines. Parameters b and m are the same for the related strip raft case and the value of parameter a is half of the related values for strip rafts.

3- 3- Curve fitting parameters

Parameters a , b , and m used in Eq. (1) were determined based on curve fitting for a specific sub-soil condition and various raft rigidities as described in previous sections. Fig. 16a shows the variation of parameter a with H/L_c for different cases presented previously based on the curve fitting procedure. As shown in this figure, a linear relationship can be drawn between parameter a and H/L_c . Therefore, parameter a can be calculated using Eq. (3):

$$a = f\left(\frac{H}{L_c}\right) = a_1\left(\frac{H}{L_c}\right) + a_2 \quad (3)$$

in which $a_1 = 2/3$ for square rafts and $a_1 = 1/3$ for strip rafts can be considered. Also, a_2 can be assumed equal to 0. If the

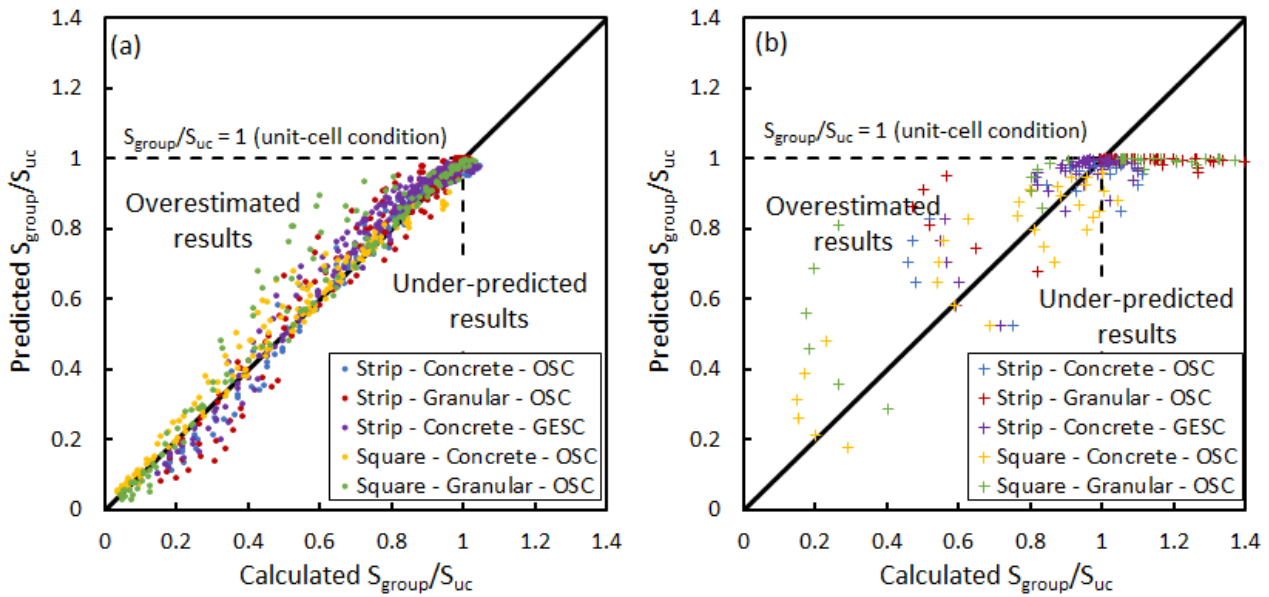


Fig. 17. Predicted vs. numerically calculated values of S_{group}/S_{uc} for square and strip, concrete and granular rafts in Bothkennar soil profile using the proposed method (a) floating groups and (b) end-bearing groups.

settlement of rafts for $L_c = 0$ having various dimensions (B) on a specific sub-soil condition was determined (numerically or analytically), the settlement ratio (settlement of finite-sized rafts without stone column, $S_{finite\ raft}$ to the settlement of infinite-sized raft, $S_{infinite\ raft}$) can be calculated. On the other hand, putting $L_c = 0$ in Eq. (2) yields:

$$\frac{S_{finite\ raft}}{S_{infinite\ raft}} = \lim_{L_c \rightarrow 0} \left(1 - \left(1 + \left(\frac{B / L_c}{f(H / L_c)} \right)^b \right)^{-m} \right) = 1 - \left(1 + \left(\frac{B}{a_1 \cdot H} \right)^b \right)^{-m} \quad (4)$$

Therefore, parameters a_1 , b and m would be calculated using iterative curve fitting of Eq. (4) with settlement ratios for $L_c = 0$. Fig. 16b shows the variation of settlement ratios for $L_c = 0$ for cases presented in Fig. 10, 12, 14, and 15 (markers) together with the fitted curve of Eq. (4) on each case. As it is shown in this figure, Eq. (4) can properly trace the trend of settlement ratios of square and strip, concrete and granular rafts without columns. Therefore, curve fitting parameters (a_1 , b , m) for another site soil can be determined using the curve fitting procedure of Eq. (4) on results of S_{group}/S_{uc} versus B for shallow rafts ($L_c = 0$); which, can be calculated analytically or using simple numerical modeling. It must be noted that curve fitting parameters (a_1 , b , m) for each case were used in previous sections.

3- 4- Assessment of the accuracy of the proposed equation

Comparison of predicted and numerically calculated values of S_{group}/S_{uc} for cases presented in Figs. 10 to 12, 14, and 15 are shown in Fig. 17. For each case, Fig. 17a shows floating SCSFs while Fig. 17b shows end-bearing SCSFs. Points above the 1:1 line indicate overestimation and points below the 1:1 line indicate under-predicted S_{group}/S_{uc} obtained from the proposed equation. Although a scattering of cases having granular rafts is more than concrete rafts, as shown in this figure, the proposed equation can predict well the S_{group}/S_{uc} of floating SCSFs, while its predictions regarding S_{group}/S_{uc} of end-bearing SCSFs are not satisfactory.

3- 5- Comparison with other methods

A comparison of the results predicted using Priebe [21] and Killeen and McCabe [26] methods with those obtained from numerical modeling in the current study is presented in Fig. 18. Since Priebe's [21] method is presented for rigid strip and square rafts and Killeen and McCabe's [26] method is developed for rigid small square rafts in the Bothkennar site, only numerical modeling results of cases with concrete square rafts are presented here. As it can be seen in this figure, Killeen and McCabe's [26] methods overestimate S_{group}/S_{uc} for large rafts (having larger values of S_{group}/S_{uc} as well) and Priebe's [21] method results are more scattered compared with the proposed method (Fig. 17). However, S_{group}/S_{uc} for end-bearing columns (plus markers) cannot be predicted suitably using any of the mentioned methods, as well as the proposed method.

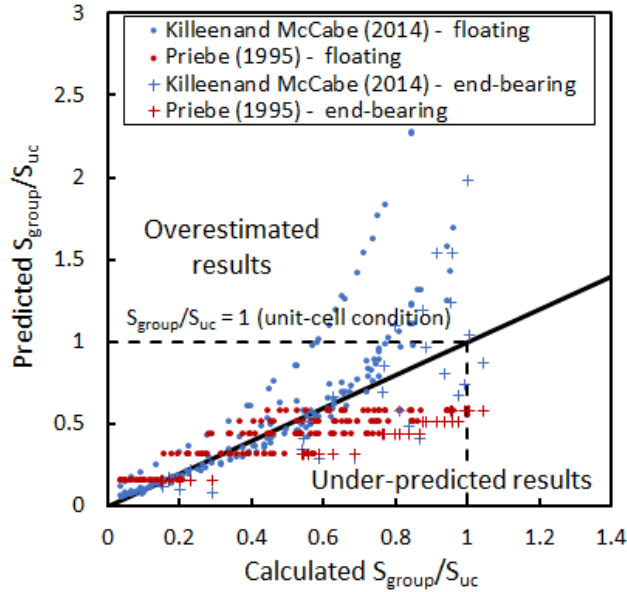


Fig. 18. Predicted vs. calculated values of S_{group}/S_{uc} for square rafts in Bothkennar soil profile using Priebe [21] and Killeen and McCabe [26] method.

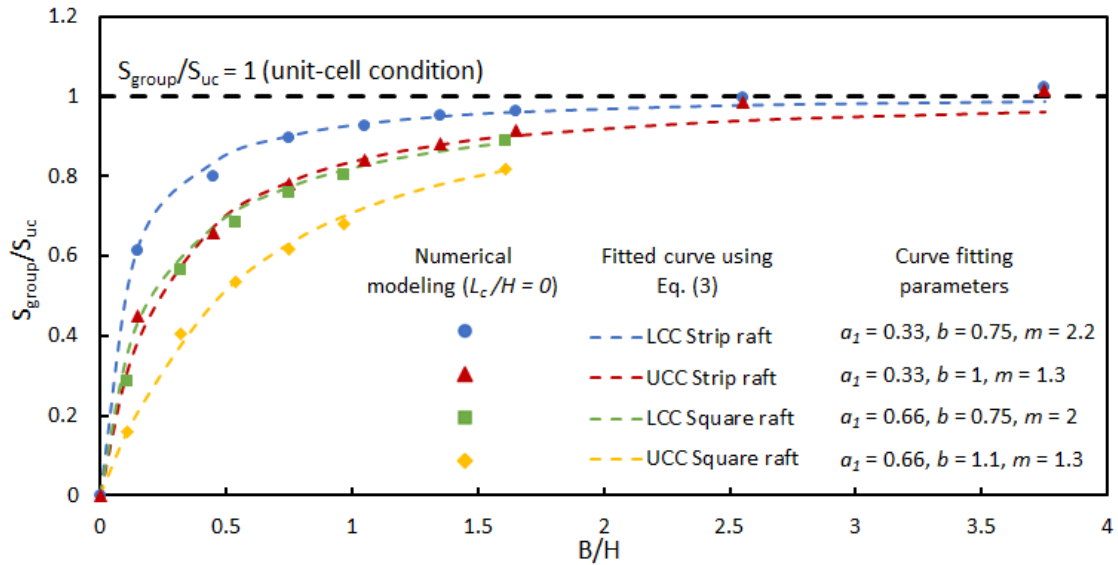


Fig. 19. Determination of curve fitting parameters for square and strip rafts in uniform native soil consisting of upper and lower Carse clay using numerically determined settlement ratio of related rafts ($L_c/H = 0$).

4- Illustrative example of using the proposed equation for other site soils

As an example of driving fitting parameters for a different sub-soil, two cases having uniform soil profiles consisting of a single layer having properties of upper and lower Carse clay layers encountered in the Bothkennar site are considered. Fitting parameters for concrete, square, and strip rafts (without stone column) are determined as shown in Fig. 19.

Comparison of settlement ratio (S_{group}/S_{uc}) predicted based on the proposed equation for floating ($L_c/H = 0.06, 0.14, 0.36, 0.57,$ and 0.79) and end-bearing column groups having $A_r = 18\%$ and various values of B together with S_{group}/S_{uc} resulted from numerical modeling are presented in Fig. 20a and b, respectively. As it is shown proposed equation can predict well S_{group}/S_{uc} for a different sub-soil condition, especially for floating groups.

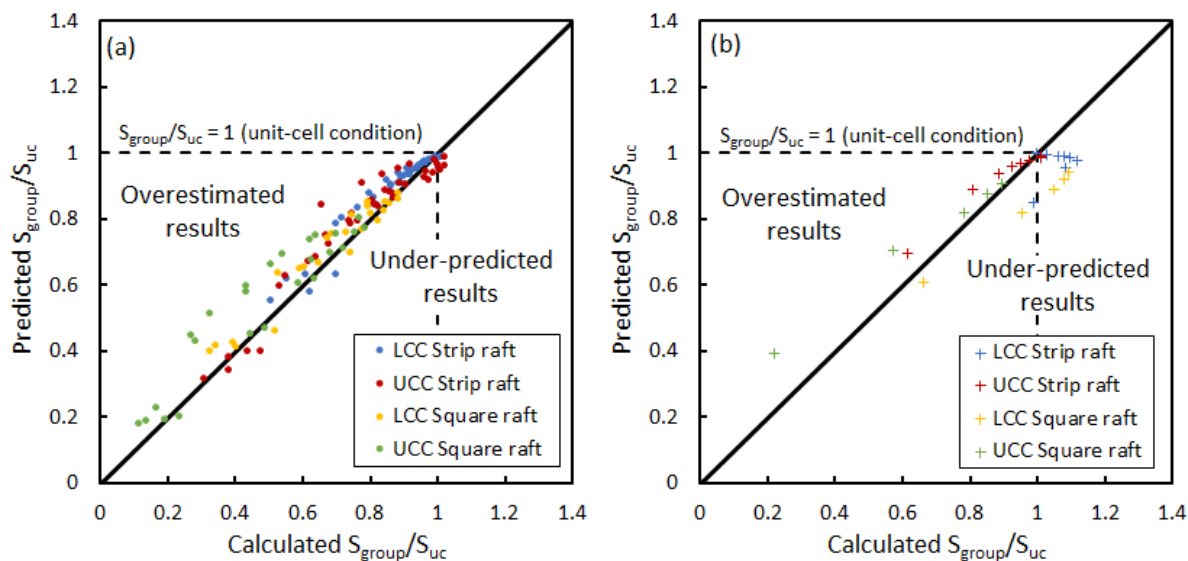


Fig. 20. Predicted vs. numerically calculated values of S_{group}/S_{uc} for square and strip rafts in uniform native soil consisting of upper and lower Carse clay (a) floating groups and (b) end-bearing groups.

5- Conclusion

Numerical modeling of a large number of stone column supported foundations (SCSFs) having various values of raft width (B), area replacement ratio (A_r), and column length (L_c), for two different raft rigidities (concrete and granular raft) and two shapes (strip and square), and two-column encasement condition (fully encased and non-encased) investigated in the current study using FEM. Results of numerical modeling of SCSFs in unit-cell condition (i.e. infinite group) compared with the results of a well-known analytical method in terms of settlement improvement factor (SIF). The existence of a good agreement between numerical modeling results and those calculated using the analytical method verifies the numerical modeling procedure of SCSFs. Moreover, numerical modeling results were also compared with two other design methods in terms of settlement ratio (S_{group}/S_{uc}) and general agreement between results observed.

A general form of the equation for determining S_{group}/S_{uc} as a function of B/L_c and H/L_c is presented and three curve fitting parameters (a , b , and m) are determined for each case of analyses; which parameters b and m are found to be constant for a specified raft rigidity and shape. Results of 5 cases including 1) strip concrete raft on OSCs, 2) strip concrete raft on GESC, 3) strip granular raft on OSCs, 4) square concrete raft on OSCs, and 5) square granular raft on OSCs show that the proposed equation can be fitted well on S_{group}/S_{uc} for SCSFs in various conditions and the function $a = f(H/L_c)$ found to be estimated using a linear equation which its slope (a_1) is about 0.33 for strip rafts and 0.66 for square rafts. Fitting parameters can be determined for another case, by fitting procedure on S_{group}/S_{uc} versus B for shallow rafts ($L_c = 0$). Variation of S_{group}/S_{uc} versus B for shallow rafts can be determined analytically or using simple numerical modeling.

A comparison of the results obtained from the proposed equation with those obtained from numerical modeling shows a good agreement for floating groups while for end-bearing groups, the accuracy of the results is not satisfactory. As indicated in sec. 3-2-4, increasing raft width has different effects on groups of floating and end-bearing columns. In floating groups increasing raft width increases settlement due to propagation of vertical stress in-depth, while in end-bearing groups (especially for higher A_r values), increasing raft width decreases settlement due to an increase in confinement and increase in column stiffness. However, one of the advantages of the proposed method compared to the existing methods is that the proposed method can be used for different raft shapes and rigidities and various sub-soil conditions.

References

- [1] F. Ou Yang, J. Zhang, W. Liao, J. Han, Y. Tang, J. Bi, Characteristics of the stress and deformation of geosynthetic-encased stone column composite ground based on large-scale model tests, *Geosynthetics International*, 24(3) (2017) 242-254.
- [2] R.S. Pugh, Settlement of floor slabs on stone columns in very soft clays, *Proceedings of the Institution of Civil Engineers-Geotechnical Engineering*, 170(1) (2017) 16-26.
- [3] M. Ghazavi, A.E. Yamchi, J.N. Afshar, Bearing capacity of horizontally layered geosynthetic reinforced stone columns, *Geotextiles and Geomembranes*, 46(3) (2018) 312-318.
- [4] B.T. Lima, M.S. Almeida, I. Hosseinpour, Field measured and simulated performance of a stone columns-strengthened soft clay deposit, *International Journal of Geotechnical Engineering*, (2019) 1-10.

- [5] I. Hosseinpour, C. Soriano, M.S. Almeida, A comparative study for the performance of encased granular columns, *Journal of Rock Mechanics and Geotechnical Engineering*, 11(2) (2019) 379-388.
- [6] A.K. Das, K. Deb, Experimental and 3D numerical study on time-dependent behavior of stone column–supported embankments, *International Journal of Geomechanics*, 18(4) (2018) 04018011.
- [7] J. Castro, C. Sagaseta, Consolidation and deformation around stone columns: Numerical evaluation of analytical solutions, *Computers and Geotechnics*, 38(3) (2011) 354-362.
- [8] S. Pal, K. Deb, Effect of clogging of stone column on drainage capacity during soil liquefaction, *Soils and Foundations*, 59(1) (2019) 196-207.
- [9] C. Cengiz, E. Güler, Seismic behavior of geosynthetic encased columns and ordinary stone columns, *Geotextiles and Geomembranes*, 46(1) (2018) 40-51.
- [10] L. Geng, L. Tang, S. Cong, X. Ling, J. Lu, Three-dimensional analysis of geosynthetic-encased granular columns for liquefaction mitigation, *Geosynthetics International*, 24(1) (2017) 45-59.
- [11] S.W. Abusharar, J. Han, Two-dimensional deep-seated slope stability analysis of embankments over stone column-improved soft clay, *Engineering Geology*, 120(1-4) (2011) 103-110.
- [12] F. Schnaid, D. Winter, A. Silva, D. Alexiew, V. Küster, Geotextile encased columns (GEC) used as pressure-relief system. Instrumented bridge abutment case study on soft soil, *Geotextiles and Geomembranes*, 45(3) (2017) 227-236.
- [13] C. Yoo, D. Lee, Performance of geogrid-encased stone columns in soft ground: full-scale load tests, *Geosynthetics International*, 19(6) (2012) 480-490.
- [14] Y. Zhou, G. Kong, Deformation analysis of geosynthetic-encased stone column–supported embankment considering radial bulging, *International Journal of Geomechanics*, 19(6) (2019) 04019057.
- [15] S. Murugesan, K. Rajagopal, Model tests on geosynthetic-encased stone columns, *Geosynthetics International*, 14(6) (2007) 346-354.
- [16] M. Samanta, R. Bhowmik, 3D numerical analysis of piled raft foundation in stone column improved soft soil, *International Journal of Geotechnical Engineering*, 13(5) (2019) 474-483.
- [17] R. Shivashankar, M.D. Babu, S. Nayak, R. Manjunath, Stone columns with vertical circumferential nails: laboratory model study, *Geotechnical and Geological Engineering*, 28(5) (2010) 695-706.
- [18] J. Black, V. Sivakumar, M. Madhav, G. Hamill, Reinforced stone columns in weak deposits: laboratory model study, *Journal of Geotechnical and Geoenvironmental Engineering*, 133(9) (2007) 1154-1161.
- [19] H. Zeydi, A. Boushehrian, Experimental and Numerical Study of Bearing Capacity of Circular Footings on Layered Soils With and Without Skirted Sand Piles, *Iranian Journal of Science and Technology, Transactions of Civil Engineering*, 44(3) (2020) 949-958.
- [20] A.K. Nazir, W.R. Azzam, Improving the bearing capacity of footing on soft clay with sand pile with/without skirts, *Alexandria Engineering Journal*, 49(4) (2010) 371-377.
- [21] H.J. Priebe, The design of Vibro replacement, *Ground engineering*, 28(10) (1995) 31.
- [22] M. Raithel, H.-G. Kempfert, Calculation models for dam foundations with geotextile coated sand columns, in: *ISRM International Symposium, OnePetro*, 2000.
- [23] J. Castro, C. Sagaseta, Influence of elastic strains during plastic deformation of encased stone columns, *Geotextiles and Geomembranes*, 37 (2013) 45-53.
- [24] Y. Zhou, G. Kong, Deformation analysis of a geosynthetic-encased stone column and surrounding soil using cavity-expansion model, *International Journal of Geomechanics*, 19(5) (2019) 04019036.
- [25] L. Keykhosropur, A. Soroush, R. Imam, 3D numerical analyses of geosynthetic encased stone columns, *Geotextiles and Geomembranes*, 35 (2012) 61-68.
- [26] M.M. Killeen, B.A. McCabe, Settlement performance of pad footings on soft clay supported by stone columns: a numerical study, *Soils and Foundations*, 54(4) (2014) 760-776.
- [27] B.A. McCabe, M.M. Killeen, Small stone-column groups: mechanisms of deformation at serviceability limit state, *International Journal of Geomechanics*, 17(5) (2017) 04016114.
- [28] S. Tabchouche, M. Mellas, M. Bouassida, On settlement prediction of soft clay reinforced by a group of stone columns, *Innovative Infrastructure Solutions*, 2(1) (2017) 1.
- [29] J. Castro, Groups of encased stone columns: Influence of column length and arrangement, *Geotextiles and Geomembranes*, 45(2) (2017) 68-80.
- [30] K.S. Ng, Settlement ratio of floating stone columns for small and large loaded areas, *Journal of GeoEngineering*, 12(2) (2017) 89-96.
- [31] J. Castro, Modeling stone columns, *Materials*, 10(7) (2017) 782.
- [32] H. Elshazly, D. Hafez, M. Mossaad, Reliability of conventional settlement evaluation for circular foundations on stone columns, *Geotechnical and Geological Engineering*, 26(3) (2008) 323-334.
- [33] N.P. Balaam, Load-settlement behavior of granular piles, Ph.D. thesis, University of Sydney, Australia, (1978).
- [34] H.G. Poulos, N.S. Mattes, Settlement of pile groups bearing on stiffer strata, *Journal of the Geotechnical Engineering Division*, 100(2) (1974) 185-190.
- [35] D. Nash, J. Powell, I. Lloyd, Initial investigations of the soft clay test site at Bothkennar, *Géotechnique*, 42(2) (1992) 163-181.
- [36] D. Hight, A. Bond, J. Legge, Characterization of the Bothkennar clay: an overview, *Géotechnique*, 42(2) (1992) 303-347.
- [37] M. Allman, J. Atkinson, Mechanical properties of reconstituted Bothkennar soil, *Géotechnique*, 42(2) (1992) 289-301.
- [38] J. Castro, Numerical modeling of stone columns beneath

- a rigid footing, *Computers and Geotechnics*, 60 (2014) 77-87.
- [39] B.G. Sexton, B.A. McCabe, Stone column effectiveness in soils with creep: a numerical study, *Geomechanics and Geoengineering*, 11(4) (2016) 252-269.
- [40] H. Shehata, T. Sorour, A. Fayed, Effect of stone column installation on soft clay behavior, *International Journal of Geotechnical Engineering*, 15(5) (2021) 530-542.
- [41] R. Brinkgreve, S. Kumarswamy, W. Swolfs, *Plaxis 3D Reference Manual Anniversary Edition Version 1*. Plaxis, Delft (2015), ISBN 978-90-76016-19-2.
- [42] M. Khabbazian, V.N. Kaliakin, C.L. Meehan, Column supported embankments with geosynthetic encased columns: validity of the unit cell concept, *Geotechnical and Geological Engineering*, 33(3) (2015) 425-442.
- [43] M.M. Killen, B. McCabe, A numerical study of factors affecting the performance of stone columns supporting rigid footings on soft clay, in: *7th European Conference on Numerical Methods in Geotechnical Engineering*, Taylor and Francis, 2010.
- [44] K. Watts, D. Johnson, L. Wood, A. Saadi, An instrumented trial of Vibro ground treatment supporting strip foundations in a variable fill, *Géotechnique*, 50(6) (2000) 699-708.
- [45] M. Elkasabgy, Performance of stone columns reinforced grounds, M.Sc. Thesis, Zagazig University, Egypt (2005).
- [46] S. Benmebarek, A. Remadna, N. Benmebarek, Numerical modeling of stone column installation effects on performance of circular footing, *International Journal of Geosynthetics and Ground Engineering*, 4(3) (2018) 1-15.
- [47] T. Schanz, P. Vermeer, P.G. Bonnier, The hardening soil model: formulation and verification, in: *Beyond 2000 in computational geotechnics*, Routledge, (2019), 281-296
- [48] B.G. Sexton, B.A. McCabe, J. Castro, Appraising stone column settlement prediction methods using finite element analyses, *Acta Geotechnica*, 9(6) (2014) 993-1011.
- [49] B.G. Sexton, B.A. McCabe, Modeling stone column installation in an elasto-viscoplastic soil, *International Journal of Geotechnical Engineering*, 9(5) (2015) 500-512.
- [50] C. Yoo, Settlement behavior of embankment on geosynthetic-encased stone column installed soft ground—a numerical investigation, *Geotextiles and Geomembranes*, 43(6) (2015) 484-492.
- [51] R. Jardine, B. Lehané, P. Smith, P. Gildea, Vertical loading experiments on rigid pad foundations at Bothkennar, *Géotechnique*, 45(4) (1995) 573-597.
- [52] B. Pulko, B. Majes, J. Logar, Geosynthetic-encased stone columns: analytical calculation model, *Geotextiles and Geomembranes*, 29(1) (2011) 29-39.
- [53] N. Balaam, J.R. Booker, Analysis of rigid rafts supported by granular piles, *International journal for numerical and analytical methods in geomechanics*, 5(4) (1981) 379-403.
- [54] R. Barksdale, R. Bachus, *Design and construction of stone columns volume I*, Federal Highway Administration Washington, DC, USA, (1983).

HOW TO CITE THIS ARTICLE

D. Ghafarian, S. M. R. Imam, Numerical Study of the Settlement of Rafts on Soft Soils Improved by Small Groups of Stone Columns, AUT J. Civil Eng., 5(4) (2021) 577-596.

DOI: [10.22060/ajce.2021.18701.5694](https://doi.org/10.22060/ajce.2021.18701.5694)



